Local-field dependence of the ^{17}O spin-lattice relaxation and echo decay rates in the mixed state of $YBa_2Cu_3O_7$

N. J. Curro,* C. Milling, J. Haase, and C. P. Slichter†
Department of Physics and Materials Research Laboratory, University of Illinois at Urbana-Champaign, 1110 West Green Street, Urbana, Illinois 61801
(Received 1 February 2000)

We find that the planar and apical ^{17}O NMR spin-lattice relaxation rate $(1/T_1)$ and the spin-echo decay rate $(1/T_2)$ are spatially dependent in the mixed state of $YBa_2Cu_3O_7$. For both sites, $1/T_1$ and $1/T_2$ increase by a factor of 2 to 3 for nuclei close to the vortex cores. The data suggest that fluctuating fields from the low-frequency vibrations of the vortex lattice give rise to the similar echo decay observed at both sites. These vibrations also dominate $1/T_1$ for both sites below $T \lesssim 25$ K. Above this temperature, the planar $1/T_1$ is dominated by spin-flip scattering with delocalized quasiparticles associated with the nodes in the superconducting gap showing that the position dependence arises from the effect of the supercurrents on the quasiparticle energy spectrum.

INTRODUCTION

Nuclear-spin-lattice relaxation is an important probe of the behavior of quasiparticle excitations in conductors and superconductors.[1,2] Strong magnetic fields or electric-field gradients can lift the degeneracy of the nuclear-spin states which then become populated according to the Boltzmann distribution. Magnetic resonance techniques (NMR, NQR) can perturb this equilibrium population distribution; by observing the time dependence of the recovery of the nuclear magnetization one can measure the spin-lattice relaxation, which is dominated in these systems by spin-flip scattering with the electrons. The only electronic states available for such processes are those close to the Fermi surface. The spin-lattice relaxation rate $1/T_1 \propto N(0)^2$, where $N(0)$ is the density of states at the Fermi level. Therefore $1/T_1$ is sensitive to processes which affect the Fermi surface, such as the development of a superconducting gap Δ_k in a superconductor. In fact, measurements of $1/T_1$ provided some of the first support of the BCS theory,[1] and more recently gave evidence that $\Delta_{\mathbf{k}}$ has nodes in $\mathbf{k}$ space in a variety of the high-temperature superconductors.[3,4]

Measurements of $1/T_1$ in the mixed state $(H_{c1} < H < H_{c2})$ of the high-temperature superconductors (HTSC's) have also provided evidence for nodes in the superconducting gap.[5–7] However, in the mixed state the vortices can have a profound influence on the spin-lattice relaxation, complicating the interpretation of $1/T_1$. Specifically, there are three properties of the vortices which can affect $1/T_1$: (i) vortex motion, which creates a time-dependent field at the nuclear site, (ii) an increase in $N(0)$ due to quasiparticle states *localized* within the vortex cores, and (iii) an increase in $N(0)$ due to *delocalized* quasiparticle states outside the vortex cores for superconductors where $\Delta_{\mathbf{k}}$ vanishes for some points in $\mathbf{k}$ space, such as in a *d*-wave superconductor. Property (i) and its effect on $1/T_1$ has been well documented in a number of conventional and high-temperature superconductors. The quasiparticle states within the vortex cores referred to in property (ii) were studied theoretically by Caroli, de Gennes, and Matricon,[8] where they point out that for an isotropically gapped superconductor there are bound states within the vortex cores with energies (with respect to E_F) $E_\mu \propto \mu/\xi^2$, where the states have orbital angular momentum $\mu\hbar$, and ξ is the coherence length, or the effective core radius. These states give a contribution $N_{\text{localized}}(0) = N_F H/H_{c2}$ to the density of quasiparticle states at the Fermi level.[9] To our knowledge, there have been no NMR measurements of this effect, however, indirect evidence for such states has been observed in conventional superconductors by surface impedance[10] and heat-capacity[11] measurements. Also, these states have been observed recently using infrared absorption,[12] and more directly using scanning tunneling microscopy.[13] The effects of property (ii), on the other hand, should be absent for $YBa_2Cu_3O_7$ and other HTSC's because the coherence length in these materials is one to two orders of magnitude smaller than in the traditional BCS *s*-wave superconductors, and thus there are many fewer states (μ) such that $E_\mu < \Delta_{\mathbf{k}}$. This observation is supported by scanning tunneling microscope measurements on $YBa_2Cu_3O_7$ which indicate that in a field of ~ 6 T there are only two states localized within the vortex cores.[14] Theoretical work also indicates that there should be few, if any states within the core of a *d*-wave vortex.[15]

The quasiparticle states associated with property (iii) are related to the *d*-wave nature of the vortices and have received attention recently because they should exist in the HTSC's. In an isotropically gapped superconductor this effect should be absent since there are no quasiparticle states with energies in the gapped region outside the vortex cores. In a *d*-wave superconductor, however, $\Delta_{\mathbf{k}}$ vanishes for $k_y = \pm k_x$. Also, for a strongly anisotropic *s*-wave superconductor, the gap may vanish for selected points in $\mathbf{k}$ space. Consequently there is no energy gap for quasiparticle states outside the core associated with these directions in $\mathbf{k}$ space. In the presence of a supercurrent, the quasiparticle spectrum is modified by a Doppler-shift term proportional to v_s, the supercurrent velocity, and as a result the density of states at the Fermi level acquires a term which is also proportional to v_s.[16] The spatial extent of these states are complicated (see Ref. 17),

however, Volovik has shown that $N_{\text{delocalized}}(0) \propto N_F\sqrt{H/H_{c2}}$.[18] A series of heat-capacity measurements on $YBa_2Cu_3O_7$ have provided support for this unusual field dependence.[16,19–21]

In this paper we present evidence for nuclear-spin-lattice relaxation associated with these unusual quasiparticle states. Measurements of the O spin-lattice relaxation in a vortex lattice in $YBa_2Cu_3O_7$ indicate that the dominant relaxation mechanism is electronic in nature. Recent work by Reyes *et al.* indicates that the spectrum of the ^{17}O central transition in $YBa_2Cu_3O_7$ exhibits the theoretical local-field distribution in a vortex lattice.[22] We confirm this result for both the apical and planar sites, and measure $1/T_1$ across the spectrum for temperatures well below the vortex lattice melting point, taking advantage of the spectral resolution to measure $1/T_1$ selectively at different local fields h ($=\nu/\gamma$, where ν is the Larmor frequency and γ is the gyromagnetic ratio) corresponding to different points in the vortex lattice. We find that $1/T_1$ increases by a factor of 2 to 3 for points close to the vortex cores (at the maxima in the local field) compared with points far from the cores (at the saddle points and minima of the local field). The local field dependence of $1/T_1$ agrees with a model in which the local density of states is proportional to the local supercurrent velocity. However, similar field dependences are also expected for a mechanism involving vortex lattice vibrations. In order to distinguish what fraction of the oxygen relaxation rate arises from vortex vibrations [property (i)] and from delocalized quasiparticles [property (iii)], we compare the temperature dependence of both sites at various spatial regions surrounding the vortex cores. For $T \gtrsim 25$ K, the planar $1/T_1$ is dominated by property (iii), whereas the apical $1/T_1$ is dominated by property (i) at all temperatures.

We also report data on the echo decay rate ($1/T_2$) across the spectrum, and find that $1/T_2$ is similar in magnitude for both sites, and increases by about a factor of 2 to 3 across the local-field distribution. These data agree with a model of collective vortex vibration with wavelength shorter than the intervortex spacing.

EXPERIMENT

The NMR data were obtained on an aligned powder of optimally doped $YBa_2Cu_3O_7$ ($T_c = 93$ K) which was isotopically enriched with ^{17}O as described in Refs. 23 and 24. The spectra, the spin-lattice relaxation, and the echo decay data were obtained using a home-built spectrometer in a field of 83 kG with $H_0 \| c$. Note that the spectra of the central transition ($+\frac{1}{2} \leftrightarrow -\frac{1}{2}$) of both the apical and the planar O sites overlap, complicating the interpretation of the spectra and relaxation data. Note that since the planar $1/T_1$ is much faster than the apical $1/T_1$ one can use a fast repetition rate to separate the contribution from the two sites. However, we found that with this method the high-frequency tail of the planar spectrum had a significant contribution from the small but nonzero signal from the apical site. Consequently, this long tail led to an underestimate of the penetration depth, which essentially determines the overall breadth of the vortex lattice line shape ($\Delta\nu \propto \phi_0/\lambda^2$, where ϕ_0 is the flux quantum, and λ is the penetration depth).

We overcome this apical overlap problem by using population enhanced double resonance[25] to resolve the central transition spectra of each site individually. Although broadened relative to their central transitions, the satellite transitions are well resolved because the two sites have different electric-field gradients ($\nu_Q^{\text{apical}} = 1.155$ MHz, $\eta^{\text{apical}} = 0$, $\nu_Q^{\text{planar}} = 0.975$ MHz, $\eta^{\text{planar}} = 0.24$). If the population difference of the first satellite transition ($+\frac{1}{2} \leftrightarrow +\frac{3}{2}$) is first inverted, the central transition population difference will be enhanced. By then taking the difference between the population enhanced spectra and the single resonance spectra, one can resolve each site and measure the relaxation rates separately. Data were taken from T_c down to 5 K. Above 60 K, the spectra were obtained by taking the Fourier transform of the echo, for a fixed satellite inversion frequency. Below 60 K, point by point spectra were obtained by sweeping both the satellite and central transition frequencies, maintaining a constant frequency difference. Below the vortex lattice melting temperature [approximately 70 K (Ref. 22)] the spectra indicate that the vortices form a well ordered solid lattice. The inset of Fig. 1 shows the evolution of the spectra from the normal state down to 5 K. The full vortex lattice line shape is not visible except for temperatures below 70 K. Above this temperature, Reyes *et al.* observed a complicated line shape which they interpreted as a combination of both frozen as well as mobile vortices. It is not clear whether this represents a phase transition (which should occur only at a specific temperature), the observation of an inhomogeneous distribution of flux lattices with a range of melting temperatures, or a combination of both apical and planar sites. Note that the temperature dependent spin shift gradually vanishes below T_c, reflecting the singlet pairing in the superconducting state.

We calculate the spectra at low temperature by approximating the local field with the London result,

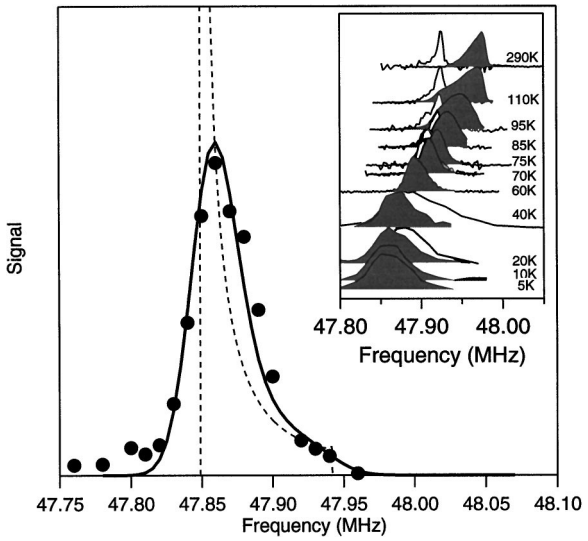

FIG. 1. The planar ^{17}O NMR spectrum of the central transition at 20 K (●). The dashed line is the theoretical spectrum, and the solid line is a fit to the convoluted expression using $\sigma = 15$ G, as described in the text. The theoretical spectrum has been adjusted so that it has the same area as the convoluted spectrum. Inset: the evolution of the planar (dark shading) and apical (no shading) spectra with temperature.

$$h(\mathbf{r}) = H_0 \sum_{m,n} \frac{e^{-Q_{mn}^2 \xi^2/2} e^{i\mathbf{Q}_{mn}\cdot\mathbf{r}}}{1+\lambda^2 Q_{mn}^2}, \quad (1)$$

where the summation is over the reciprocal lattice vectors of a triangular lattice. The expression for the local field used here includes a cutoff at low wavelengths.[26,27] Here ξ is the coherence length, H_0 is the applied field,

$$\mathbf{Q}_{m,n} = \left(\frac{2\pi^2 H_0}{\sqrt{3}\phi_0}\right)^{1/2} (\sqrt{3}n, 2m-n), \quad (2)$$

and m and n are integers. The NMR spectrum, determined by the number of nuclei resonating at a particular local field, is given by the local-field distribution:

$$f(h) = \int_\Omega \delta[h(\mathbf{r}) - h] d^2\mathbf{r}, \quad (3)$$

where Ω is the unit cell. The theoretical spectrum was then convoluted with a Gaussian broadening function, given by $f(x) = e^{-x^2/2\sigma^2}$, where σ was varied, and ξ and λ were fixed at 15 and 1600 Å, respectively. Figure 1 shows the spectra at 20 K, and compares the data with a calculation for the central transition. The value of 1600 Å for the penetration depth agrees with other measurements.[28] Note that the low-field (frequency) part of the spectrum corresponds to nuclei far from the vortex cores, the high-field part corresponds to nuclei close to the cores, and the peak in the spectrum corresponds to nuclei near the saddle points in the local-field distribution.

The spin-lattice relaxation data were obtained by measuring single resonance echo integrals on the satellite transition to eliminate baseline signal from the apex and chain oxygen sites. The magnetization recovery data fit the expected normal-modes recovery function for a spin-$\frac{5}{2}$ nucleus undergoing magnetic relaxation. The satellite spectrum has poorer resolution than the central transition, however the vortex lattice line shape remains well defined. The excitation bandwidth at the central transition (see Fig. 1) of $H_1 \sim 10$ kHz was significantly smaller than the linewidth. The spin-lattice relaxation rate versus frequency (or local field) is shown in Fig. 2 for a series of temperatures. Note that $1/T_1$ increases by a factor of about 2 to 3 across the spectra for all temperatures and for both sites. At 40 K, the spin-lattice relaxation was measured using the population enhanced double resonance by varying the time t between the inversion pulse on the satellite and the echo sequence on the central transition using the following pulse sequence: $(\pi)_{\text{sat}}$-t-$(\pi/2)_{\text{cen}}$-τ-$(\pi)_{\text{cen}}$-echo. The magnetization enhancement of the central transition is then given by: $M(t) = M_0$ $(\frac{25}{21}e^{-15t/T_1} - \frac{2}{15}e^{-6t/T_1} - \frac{2}{35}e^{-t/T_1})$.

Note that the planar site spectra in the normal state (see the inset of Fig. 1) reveal a low-frequency temperature-dependent tail, which may be an indication of doping inhomogeneity in the sample. When $YBa_2Cu_3O_7$ is isotopically enriched with ^{17}O, sample doping homogeneity can be degraded.[29] Evidence for a slight inhomogeneity can also be seen in both the Cu NQR spectrum and the diamagnetic response at T_c measured by dc superconducting quantum interference device, both of which are broadened relative to nonenriched materials.[23] The effect of this doping inhomogeneity on the relaxation rate in the vortex state should be minimal since the differences in magnetic shifts go to zero at the relevant temperatures for the experiments. Furthermore, the doping dependence of T_1 also vanishes at low temperatures;[30] at 47 K, $^{17}T_1^{-1}$ for $YBa_2Cu_3O_{6.96}$ is only 7–8% greater than $^{17}T_1^{-1}$ for $YBa_2Cu_3O_{6.67}$. The T_1 variation across the vortex line is two orders of magnitude greater, and is likely unrelated to the doping inhomogeneity.

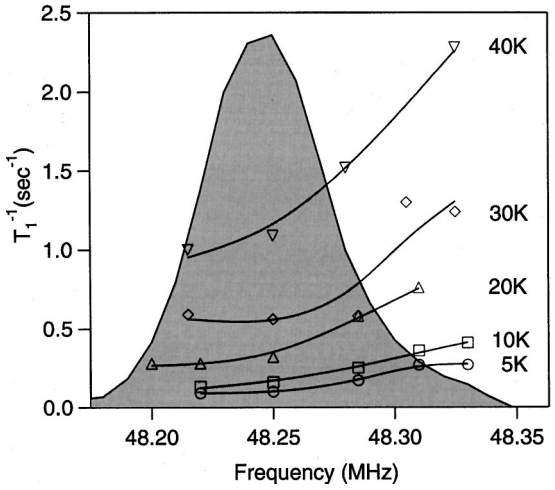

FIG. 2. The planar oxygen spin-lattice relaxation rate as a function of frequency across the satellite transition. The solid lines are guides to the eye, and the error is represented by the data point sizes. The shaded region is the spectrum at 40 K.

The spin-echo decay was measured on the central transition by keeping t fixed and varying τ. The data were well approximated by an exponential over one and a half decades, and were fit to the form $M(2\tau) = M_0 e^{-2\tau/T_2}$. The frequency dependences of $1/T_2$ for both sites are shown in Fig. 3 for a series of temperatures. At the peak in the spectrum, the mag-

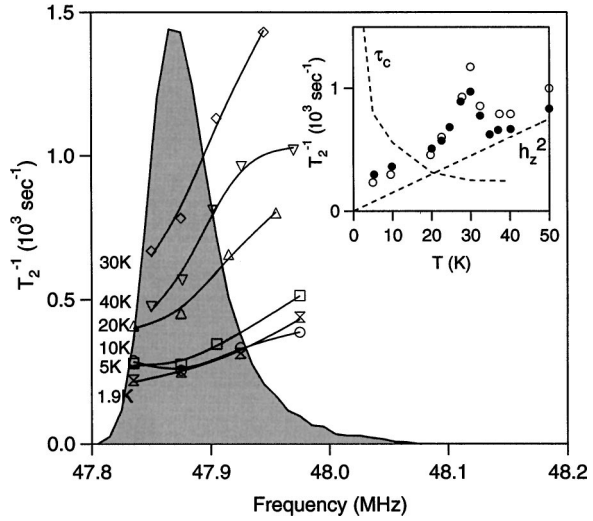

FIG. 3. The planar spin-echo decay rate across the central transition. The solid lines are guides to the eye. The shaded area is the spectrum at 10 K. The error is represented by the size of the data points. Inset: the temperature dependence of $1/T_2$ for both the planar (●) and apical (○) sites, as well as $\langle h_z^2 \rangle$ and τ_c, as discussed in the text.

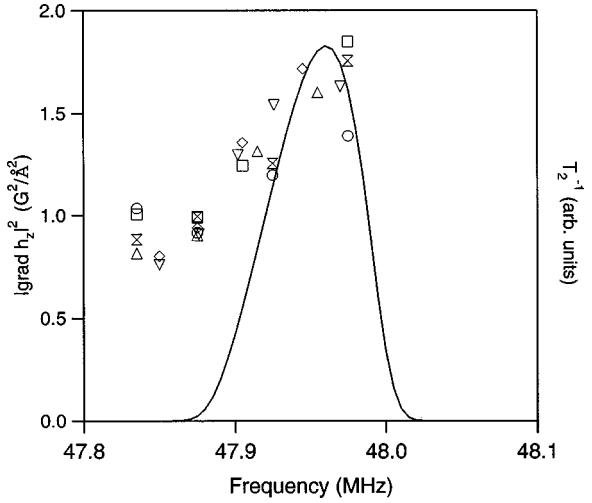

FIG. 4. The scaled echo decay rates of the planar site. The symbols are the same as in Fig. 3. The $1/T_2$ scaling factor ratios are (in descending temperatures) 4:3:5:9:9:10. The solid line is the theoretical $1/T_2$ distribution as discussed in the text.

nitude of the planar $1/T_2$ is of the same order (about 25–30% greater) as reported by Recchia *et al.*[31] We likewise observe a peak in the echo decay rate at approximately 30 K for both sites. The temperature dependence of the $1/T_2$ is shown in the inset of Fig. 3 for both sites at the peak in the spectra. Figure 4 shows the O echo decay rate data versus frequency, in which the data have been scaled at all temperatures to indicate the similar local-field dependence.

DISCUSSION

The local-field dependence of $1/T_1$ and $1/T_2$ is striking, and seems to indicate a strong influence of the vortex lattice. We first discuss the echo decay data. In the normal state, Recchia *et al.*[31] found that the mechanism for the echo decay of the planar oxygen arises from fluctuating local dipolar (direct and indirect) fields at the oxygen site from the nearest-neighbor copper nuclei, which undergo fast nuclear-spin fluctuations. Thus the O echo decay is entirely determined by the Cu T_1 in the normal state. However, in the superconducting mixed state there is a second decay mechanism that is much faster than that which the Cu T_1 mechanism predicts. Due to the particular frequency dependence of $1/T_2$ seen in Fig. 3 one might conclude that motion of the vortex lattice is in fact the cause of the extra relaxation below the melting temperature. In fact, the similar behavior of both the apical and planar sites supports this hypothesis, since the local vortex lattice motion should produce the same time-dependent field at both sites.

In order to estimate the effect of vortex lattice motion on the echo decay, we assume that the extra relaxation arises from a fluctuating field $h_z(t)$ with a correlation function

$$\langle h_z(t)h_z(0)\rangle = \langle h_z^2\rangle e^{-t/\tau_c}. \tag{4}$$

Then, in the limit of $\tau_c \ll t$, the time of the spin-echo experiment, the decay is exponential with time constant

$$\frac{1}{T_2} = {}^{17}\gamma^2 \langle h_z^2\rangle \tau_c. \tag{5}$$

Let us postulate that the fluctuations arise from some collective motion of the vortex lattice. At nonzero temperatures the vibrational modes of the vortex lattice can be thermally excited in much the same manner as the phonon modes of a crystal lattice. The three principle modes that can be excited consist of a shear wave, a tilt wave, and a compression wave of the lattice, however, compression modes usually have much higher frequencies than the other two. Bulaevskii *et al.*[33] have discussed these vibrations for an unpinned lattice. They show that the maximum frequencies of the shear and tilt waves are $\omega_s \approx H_0\phi_0/16\pi\lambda^2\eta$ and $\omega_t \approx \phi_0^2/32\pi\lambda^4\eta$, respectively, where η is the Bardeen-Stephan constant which represents a drag term acting on a moving vortex. For conventional superconductors, η is given by $\eta = \phi_0^2/2\pi\xi^2\rho_n c^2$, where ρ_n is the normal-state resistivity. Thus for the typical parameters in the experiment ($H_0 = 83$ kG, $\rho_n \sim 100\,u\Omega$ cm), $\tau_s = 1/\omega_s \sim 10^{-12}$ sec and $\tau_t = 1/\omega_t \sim 10^{-10}$ sec.

Furthermore, Bulaevskii *et al.* point out that the vortices undergo overdamped motion, with a correlation function given by

$$\langle s^2(t)\rangle = s_0^2 \frac{k_B T}{\varepsilon_{s,t}} e^{-t/\tau_{s,t}}, \tag{6}$$

where $\langle s^2\rangle$ is the mean-squared displacement of a vortex, s_0^2 is a constant, and $\varepsilon_{s,t}$ is the elastic energy of the particular mode. The local-field fluctuation can be approximated by $\langle h_z^2(\mathbf{r})\rangle \approx |\nabla h(\mathbf{r})\cdot\mathbf{s}(\mathbf{r})|^2$, where $\mathbf{s}(\mathbf{r})$ is the local displacement vector of the vortex lattice at $\mathbf{r}$. Assuming a common correlation time for all points in the lattice, i.e.,

$$\tau_c = \tau_{s,t}, \tag{7}$$

and that $s(\mathbf{r})$ varies in space with wavelengths large compared with the intervortex spacing L ($L \sim 170$ Å at 83 kG) [note, however, that the magnitude of $s(\mathbf{r})$ itself must remain small], this leads one to the conclusion that

$$\langle h_z^2\rangle \propto |\nabla h(\mathbf{r})|^2 T. \tag{8}$$

The frequency dependence of $1/T_2$ across the vortex lattice line shape should then be given approximately by $|\nabla h(\mathbf{r})|^2$ versus $\gamma h(\mathbf{r})$.

Figure 4 compares the T_2 distribution calculated in this manner with the experimental data. The calculated $1/T_2$ distribution has been convoluted with the same Gaussian broadening function which was used to fit the spectrum. Note that the decrease in $1/T_2$ at the upper end of the spectrum arises from the vanishing gradient of the local field at the cores in the model taken in Eq. (1). The data have all been scaled to fall along the same line, and exhibit a trend similar to the theoretical prediction. However, they do not vanish at low frequencies as the theory would predict. If the vortex lattice underwent displacements (perpendicular to the axis of the core) with wavelengths (λ_V) large with respect to L, then the local-field fluctuations would vanish for points close to the saddle point of the local-field distribution. The saddle point corresponds to the peak at low frequency in the vortex lattice line shape. If, on the other hand, there are displacements

such that $\lambda_V \sim L$, then the local field fluctuations need not vanish at the saddle points. The data seem to support the latter picture.

It is interesting to note that in order to explain the magnitude of $1/T_2$ using the values given above for $\tau_{s,t}$ one requires a fluctuating field $h_z \sim 10^5$ G, which is unphysical. One explanation is that η is significantly larger in a pinned vortex lattice. Furthermore, one might expect that the effective viscosity in a pinned lattice would increase with decreasing temperature, as fewer and fewer vortices have enough thermal energy to overcome the pinning energies. This leads to a natural explanation of the peak in $1/T_2$ at 30 K, since h_z^2 decreases with decreasing temperature and $\tau_c \propto \eta$ increases with decreasing temperature. Therefore the product of these two functions could have a peak at some intermediate temperature. Furthermore, combining Eqs. (5)–(8), we find the temperature dependence of τ_c is given by

$$\tau_c \sim 1/T_2 T. \tag{9}$$

We show the temperature dependence of h_z^2 and τ_c calculated in this manner in the inset of Fig. 3. Note that for physically reasonable fluctuating fields (on the order of 1 G), one requires $\tau_c \sim 10^{-6}$ sec, or that η is some four to five orders of magnitude greater in the pinned lattice. Recchia *et al.* reached a similar conclusion, in which they find that the vortex motion near the melting temperature appears to be six orders of magnitude slower than predictions from numerical simulations on an unpinned lattice.[31]

Note, however, that the peak in $1/T_2$ at 30 K may be unrelated to the vortex lattice motion. A T_2 peak for Cu in zero field has been observed by various authors and was recently related to a charge ordering transition.[32] Low-frequency fluctuations in the local electric-field gradient could contribute to the T_2 of both the planar and apical oxygens, and would be independent of local position in the vortex lattice.

We now turn to the analysis of the spin-lattice relaxation data. In general the oxygen spin-lattice relaxation rate is composed of a contribution from vortex motion and a contribution from scattering from quasiparticles:

$$\frac{1}{T_{1,\mathrm{expt}}} = \frac{1}{T_{1,\mathrm{qps}}} + \frac{1}{T_{1,\mathrm{vm}}}. \tag{10}$$

It is useful to compare the T_1 of the oxygen with the T_1 of the copper. If there is a contribution due to vortex motion, then the ratio of these contributions should be given by $^{63}T_{1,\mathrm{vm}}^{-1}/^{17}T_{1,\mathrm{vm}}^{-1} = (^{63}\gamma/^{17}\gamma)^2 = 3.82$. The experimental ratio at low temperature is 10 at 83 kG.[23,24] This means that there must be a significant quasiparticle contribution to the T_1 of the Cu, and possibly to the O. In a similar manner, if the T_1's of the two oxygen sites are determined by vortex fluctuations, then their T_1's should be the same. So in the temperature range where they differ substantially, the O with the faster T_1 cannot be dominated by the vortex vibrations. Examination of Fig. 5 shows that above 25 K, the planar O T_1 is substantially faster than that of the apical and has a different temperature dependence (T^3 rather than T). Therefore its T_1 cannot be due to vortex vibrations in this temperature range. Below 25 K, the T_1's still differ by a factor of 2.5, but both T_1's have the same linear temperature dependence. Possibly the relaxation at the planar site is still not entirely from vortex vibrations, but we cannot be as sure that the factor of 2.5 does not arise because at the microscopic level there is a small difference in fluctuating vortex fields at the planar and apical sites.

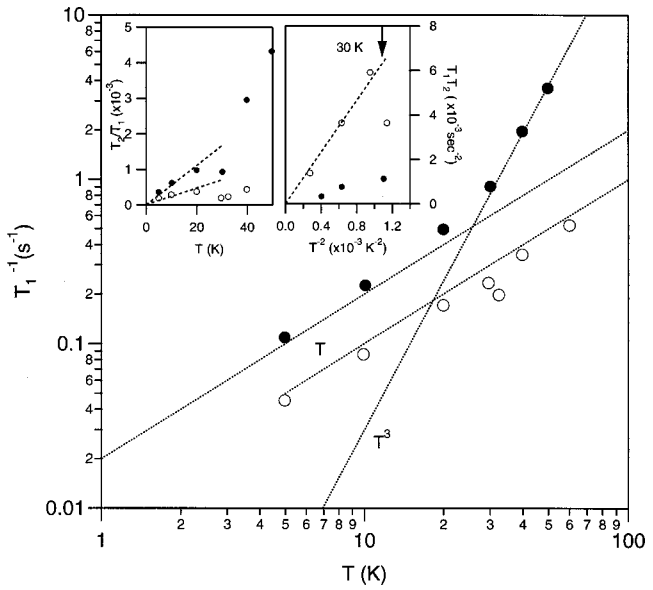

FIG. 5. $1/T_1$ versus T for the planar (●) and the apical (○) sites at the peak frequencies in their respective spectra. Inset: (left panel) T_2/T_1 versus T, and (right panel) T_1T_2 versus T^{-2}.

If the T_1 of the O is entirely determined by vortex motion, then we have[2]

$$\frac{1}{T_{1,\mathrm{vm}}} = \gamma^2 h_\perp^2 \frac{\tau_c}{1+\omega_L^2\tau_c^2}, \tag{11}$$

where ω_L is the Larmor frequency and $h_\perp$ is the fluctuating field (proportional to T) in the perpendicular direction. Note, however, that vortex vibrations are likely to strongly affect the fluctuating field along the static field direction (h_z), but not the perpendicular fluctuating field ($h_\perp$). Therefore one would expect T_1 to be less sensitive to vortex vibrations than T_2. Let us consider the case $\omega_L\tau_c \ll 1$. Then $1/T_1 = \gamma^2 h_\perp^2 \tau_c$, which is identical to the form for T_2, except for the amplitude of the fluctuating field in the perpendicular direction. However, this amplitude should have the same temperature dependence as the longitudinal field, and hence $1/T_1$ and $1/T_2$ should have identical temperature dependences. Examination of the insert in Fig. 5 shows that they do not, and so if $1/T_1$ arises entirely from vortex vibrations, $\tau_c \gg 1/\omega_L$ and $1/T_1 \approx \gamma^2 h_\perp^2/\omega_L^2\tau_c \sim T/\tau_c$. These expressions should hold true from 40 K down. Note that estimates of the magnitude of $1/T_2$ also support this conclusion. Furthermore, for sufficiently large $\tau_c \sim 1/\gamma h_z$, $T_2 = \tau_c$. This suggests that the peak in $1/T_2$ at 30 K occurs when this condition is met. Therefore above 30 K, $T_1T_2 \sim T^{-2}$ is independent of τ_c, and below 30 K, $T_2/T_1 \sim T$ is independent of τ_c. These quantities are shown in the inset of Fig. 5. The relations appear to hold for the apical O, but not for the planar O above 25 K. In Fig. 5 we show the temperature dependence of $1/T_1$ for both sites at the peak intensity of the absorption curves. Note that $T_{1,\mathrm{planar}}^{-1} \sim T^3$ for $T \gtrsim 25$ K; below this temperature $T_{1,\mathrm{planar}}^{-1}$

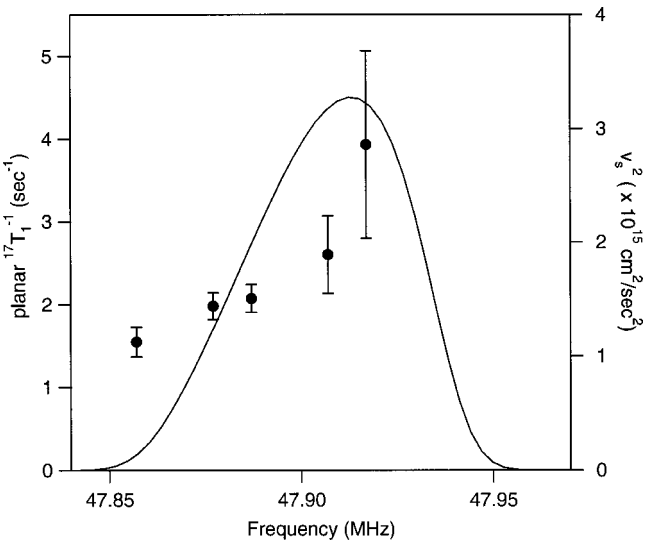

FIG. 6. The spin-lattice relaxation rate distribution. The data points (●) are the planar T_1^{-1} data points at 40 K measured on the central transition using the population enhancement technique as described in the text, and the solid line is the calculated v_s^2 distribution, convoluted with a broadening function with width $\sigma = 15$ G.

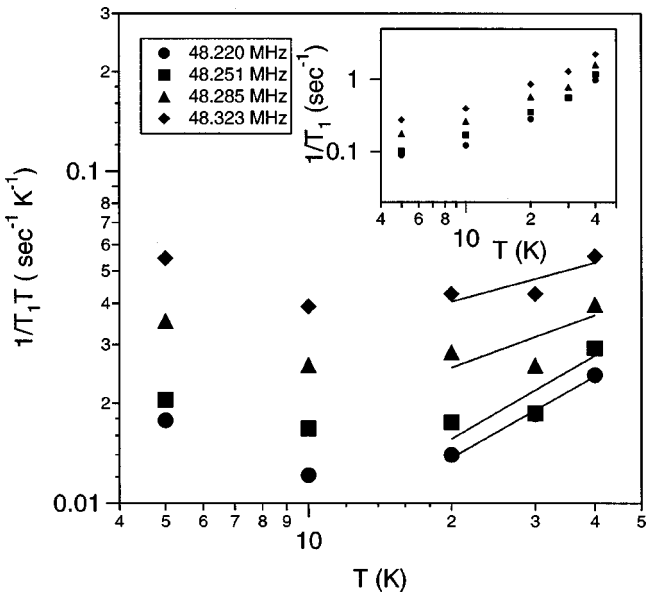

FIG. 7. $1/T_1T$ versus T and (Inset) $1/T_1$ versus T for four points across the vortex lattice spectrum. For frequencies at which no data points exist, smoothly interpolated values were used. The solid lines are best fits to the data in the range $20 < T < 40$ K.

$\sim T$. On the other hand, $T_{1,\text{apical}}^{-1} \sim T$ over the entire temperature range. For vortex lattice motion, one might expect a linear temperature dependence since $h_\perp^2 \sim T$, however, for an electronic mechanism a T^3 dependence is expected. Therefore the data seem to suggest that the spin-lattice relaxation of the apical O is dominated primarily by vortex lattice motion, whereas for $25 \lesssim T \lesssim 70$ K, the spin-lattice relaxation of the planar O is dominated by an electronic mechanism. We are not sure what the mechanism is for the planar O for temperatures below 25 K.

Let us consider the term arising from scattering with the quasiparticles. In the absence of a field, the energy of a quasiparticle excitation in the BCS framework is

$$E_{\mathbf{k}} = \sqrt{\varepsilon_{\mathbf{k}}^2 + \Delta_{\mathbf{k}}^2}, \tag{12}$$

where $\varepsilon_{\mathbf{k}}$ is the quasiparticle energy in the normal state. However, in the presence of a supercurrent this spectrum is modified by a Doppler shift term:[26]

$$E_{\mathbf{k}} = \sqrt{\varepsilon_{\mathbf{k}}^2 + \Delta_{\mathbf{k}}^2} + \hbar \mathbf{k}_F \cdot \mathbf{v}_s, \tag{13}$$

where v_s is the supercurrent velocity and $\mathbf{k}_F$ is the Fermi wave vector. In a superconductor with an isotropic gap, this term is unimportant except when the supercurrent is close to the critical current. However, in a superconductor with lines of nodes in the gap the Doppler shift term becomes important for $\mathbf{k}_F$ close to the gap nodes, in which case $N(0) \sim v_s(\mathbf{r})$.[16] Roughly, one would expect then that $1/T_{1,\text{qps}} \sim v_s^2(\mathbf{r})$. In the mixed state v_s circulates around the vortices. Thus $1/T_1$ should have the same periodicity, with a maximum close to the vortex cores, and a minimum for points far from the cores.

Note, however, it is important to take into account the relative magnitudes of (i) k_BT, (ii) the Zeeman energy of the scattered quasiparticle, and (iii) the Doppler-shift term, which varies with position in the vortex lattice. As a result, theoretical expressions for the quasiparticle contribution to $1/T_1$ can be quite complex. Wortis, Berlinsky, and Kallin have calculated the quasiparticle and vortex motion contributions to the Cu T_1.[34] Also, Morr, and Wortis[35] have calculated the Cu T_1 using a spin-fermion, strong-coupling model. Concurrently, Takigawa, Ichioka, and Machida[36] have determined the position dependent local density of states and T_1 by solving the Bogoliubov–de Gennes equation. In all theoretical treatments, the Cu T_1 increases for points close to the vortex cores, as seen experimentally. Preliminary calculations for the O T_1 indicate a similar position dependence.[37]

For concreteness, we estimate the frequency dependence of $1/T_1$ for the O by assuming that $1/T_{1,\text{qps}} \propto v_s^2$, and

$$v_s^2 = (J_s/n_s e)^2 = \left(\frac{c}{4\pi n_s e}\right)^2 |\nabla \times h(\mathbf{r})|^2, \tag{14}$$

where n_s is the superconducting condensate density. Thus the frequency dependence of $1/T_1$ should be given approximately by $v_s^2(\mathbf{r})$ versus $\gamma h(\mathbf{r})$. This distribution is shown in Fig. 6 for a system using the same parameters as used to fit the spectrum, and compared with the T_1 data at 5 K. The density n_s was estimated using the relation $\lambda^2 = mc^2/4\pi n_s e^2$, where m is the electron mass, and e is the electron charge. The decrease in the v_s^2 distribution at high frequency reflects the vanishing of the curl of the local field in the model taken in Eq. (1). Note that the quasiparticle contribution to $1/T_1$ of a superconductor with an isotropic gap, on the other hand, would have no local-field dependence.

A further prediction of the theory is that $1/T_1$ should contain a term proportional to $v_s^2 T$ at low temperatures in addition to the T^3 term expected in zero applied field.[35] (Note that by symmetry one can exclude terms linear and cubic in v_s.) At low temperatures, then, $1/T_1T$ should become independent of T for points close to the vortex cores where v_s is

largest but have a T^2 dependence far from the core. Figure 7 shows the temperature dependence of $1/T_1T$ for various points across the vortex lattice spectrum. Note that for $20 < T < 40$ K, where the electronic mechanism dominates, $1/T_1T$ varies strongly with T at lower frequencies but approaches a constant value at higher frequencies, as expected.

CONCLUSIONS

In the mixed state of $YBa_2Cu_3O_7$, we find that the planar and apical ^{17}O spin-lattice relaxation rate and the spin-echo decay rate are spatially dependent with the period of the vortex lattice. Both $1/T_1$ and $1/T_2$ increase by a factor of 2 to 3 for nuclei close to the vortex cores. We interpret the echo decay of both nuclei as arising from fluctuating fields from vibrations of the vortex lattice with displacement wavelengths $\lambda_V < L$, and correlation times on the order of 10^{-6} sec. Estimates for the correlation time of an unpinned vortex lattice, however, are four to six orders of magnitude faster. The discrepancy may be understood if one concludes that the drag term η acting on a moving vortex in a *pinned* lattice is four orders of magnitude greater than estimates based on the Bardeen-Stephan constant. The spin-lattice relaxation rate of the apical O is dominated by vortex lattice motion. Above 25 K, the spin-lattice relaxation of the planar O is dominated by an electronic contribution, whose local-field dependence agrees qualitatively with the effect expected for spin-flip scattering with delocalized quasiparticles outside of the vortex cores.

ACKNOWLEDGMENTS

We are grateful to D. Pines for first pointing out this problem to us, as well as R. Wortis, D. Morr, A. Sokol, R. Stern, and D. Smith for many valuable and stimulating discussions, and also K. Machida for communicating their work to us. This work has been supported by the National Science Foundation Grant No. (DMR 91-20000) through the Science and Technology Center for Superconductivity and by the U.S. Department of Energy, Division of Materials Science Grant No. DEFG 02-96ER45439 through the University of Illinois at Urbana-Champaign, Frederick Seitz Materials Research Laboratory. J.H. acknowledges support by the Deutsche Forschungsgemeinschaft.

*Present address: Los Alamos National Laboratory, Los Alamos, NM 87545.

†Also at Department of Chemistry, University of Illinois at Urbana-Champaign.

[1] L. C. Hebel and C. P. Slichter, Phys. Rev. **113**, 1504 (1957).

[2] C. P. Slichter, *Principles of Magnetic Resonance*, 3rd ed. (Springer Verlag, New York, 1990).

[3] T. Imai, T. Shimizu, T. Tsuda, H. Yasuoka, T. Takabatake, Y. Nakazawa, and M. Ishikawa, J. Phys. Soc. Jpn. **57**, 1771 (1988).

[4] Takashi Imai, Ph.D. thesis, Institute for Solid State Physics, The University of Tokyo, 1991.

[5] J. A. Martindale, S. E. Barrett, D. J. Durand, K. E. O'Hara, C. P. Slichter, W. C. Lee, and D. M. Ginsberg, Phys. Rev. B **50**, 13 645 (1994).

[6] N. Bulut and D. Scalapino, Phys. Rev. Lett. **67**, 2898 (1991).

[7] D. Thelen, D. Pines, and J. P. Lu, Phys. Rev. B **47**, 9151 (1993).

[8] C. Caroli, P. de Gennes, and J. Matricon, Phys. Lett. **9**, 307 (1964).

[9] A. L. Fetter and P. C. Hohenberg, *Superconductivity*, edited by R. D. Parks (Marcel Dekker, New York, 1969), pp. 817–924.

[10] B. Rosenblum and M. Cardona, Phys. Rev. Lett. **12**, 657 (1964).

[11] J. Ferreira da Silva, E. A. Burgmeister, and Z. Dokonpil, Physica A **41**, 409 (1969).

[12] K. Karrai, E. J. Choi, F. Dunmore, S. Liu, H. D. Drew, Q. L. Li, D. B. Fenner, Y. D. Zhu, and F-C. Zhang, Phys. Rev. Lett. **69**, 152 (1992).

[13] H. F. Hess, R. B. Robinson, and J. M. Waszezak, Phys. Rev. Lett. **64**, 2711 (1990).

[14] I. Maggio-Aprile, Ch. Renner, A. Erb, E. Walker, and Ø. Fisher, Phys. Rev. Lett. **75**, 2754 (1995).

[15] M. Franz and Z. Tešanović, Phys. Rev. Lett. **80**, 4763 (1998).

[16] K. Moler, D. Sisson, J. Urbach, M. Beasley, A. Kapitulnik, D. Baar, R. Liang, and W. Hardy, Phys. Rev. B **55**, 3954 (1997).

[17] A. S. Mel'nikov, cond-mat/9806188 (unpublished).

[18] G. E. Volovik, Pis'ma Zh. Eksp. Teor. Fiz. **58**, 457 (1993) [JETP Lett. **58**, 469 (1993)].

[19] K. Moler, D. Baar, J. Urbach, R. Liang, W. Hardy, and A. Kapitulnik, Phys. Rev. Lett. **73**, 2744 (1994).

[20] N. E. Phillips, R. A. Fisher, and J. E. Gordon, in *Progress in Low Temperature Physics*, edited by D. F. Brewer (Elsevier Science, Amsterdam, 1997), Vol. 13, pp. 267–357.

[21] B. Revaz, J.-Y. Genoud, A. Junol, K. Neumaier, A. Erb, and E. Walker, Phys. Rev. Lett. **80**, 3364 (1998).

[22] A. P. Reyes, X. P. Tang, H. N. Bachman, W. P. Halperin, J. A. Martindale, and P. C. Hammel, Phys. Rev. B **55**, R14 737 (1997).

[23] J. A. Martindale, Ph.D. thesis, The Univesity of Illinois, Urbana, IL, 1991.

[24] J. A. Martindale, S. E. Barrett, K. E. O'Hara, C. P. Slichter, W. C. Lee, and D. M. Ginsberg, Phys. Rev. B **47**, 9155 (1993).

[25] J. Haase, N. J. Curro, R. Stern, and C. P. Slichter, Phys. Rev. Lett. **81**, 1489 (1998).

[26] M. Tinkham, *Introduction to Superconductivity* (Robert E. Krieger, Malabar, FL, 1975).

[27] E. H. Brandt, Phys. Status Solidi B **51**, 345 (1972).

[28] W. N. Hardy, D. A. Bonn, D. C. Morgan, R. Liang, and K. Zhang, Phys. Rev. Lett. **70**, 3999 (1993).

[29] M. Horvatic, Y. Berthier, P. Butaud, Y. Kitaoka, P. Segransan, C. Berthier, H. Katayama-Yoshida, Y. Okabe, and T. Takahashi, Physica C **159**, 689 (1989).

[30] J. A. Martindale, P. C. Hammel, W. L. Hults, and J. L. Smith, Phys. Rev. B **57**, 11 769 (1998).

[31] C. Recchia, J. H. Martindale, C. H. Pennington, W. L. Hults, and J. L. Smith, Phys. Rev. Lett. **78**, 3543 (1997).

[32] S. Krämer and M. Mehring, Phys. Rev. Lett. **83**, 396 (1999).

[33] L. N. Bulaevskii, N. N. Kolesnikov, I. F. Shegolev, and O. M. Vyaselev, Phys. Rev. Lett. **71**, 1891 (1993).

[34] R. Wortis, A. J. Berlinsky, and C. Kallin, Phys. Rev. B **61**, 12 342 (2000).

[35] D. K. Morr and R. Wortis, Phys. Rev. B **61**, R882 (2000).

[36] M. Takigawa, M. K. Ichioka, and K. Machida, Phys. Rev. Lett. **83**, 3057 (1999).

[37] D. K. Morr (private communication).